

NASA TECHNICAL NOTE



NASA TN D-2649

NASA TN D-2649

AMPTIAC

59148

# GRAIN GROWTH IN DILUTE TUNGSTEN-BORON ALLOYS

*by Peter L. Raffo*

*Lewis Research Center  
Cleveland, Ohio*

*and*

*Robert F. Hehemann*

*Case Institute of Technology  
Cleveland, Ohio*

**DISTRIBUTION STATEMENT A**  
Approved for Public Release  
Distribution Unlimited

REPRODUCED FROM  
BEST AVAILABLE COPY

20010920 096

GRAIN GROWTH IN DILUTE TUNGSTEN-BORON ALLOYS

By Peter L. Raffo

Lewis Research Center  
Cleveland, Ohio

and

Robert F. Hehemann

Case Institute of Technology  
Cleveland, Ohio

NATIONAL AERONAUTICS AND SPACE ADMINISTRATION

---

For sale by the Office of Technical Services, Department of Commerce,  
Washington, D.C. 20230 -- Price \$1.00

TERRA

## GRAIN GROWTH IN DILUTE TUNGSTEN-BORON ALLOYS

by Peter L. Raffo and Robert F. Hehemann

Lewis Research Center

### SUMMARY

The grain-growth behavior of arc-melted tungsten and several binary tungsten-boron alloys (0.005 to 0.67 atomic percent B) was studied in the temperature range 3600° to 4200° F. The alloys were prepared by arc melting sintered electrodes of tungsten and elemental boron powders, followed by extrusion and swaging. Specimens cut from the swaged rod were recrystallized at 3200° F to insure that only grain growth would take place in the subsequent annealing treatments.

The grain-growth kinetics were followed by measuring the decrease in grain-boundary surface area  $\beta$  as a function of time at temperature. At 3600° and 3800° F, the decrease in  $\beta$  obeyed a power law of the form  $\beta = kt^{-n}$ , where  $t$  is time and  $n$  and  $k$  are constants. At 4000° and 4200° F, however, the power law was no longer obeyed because of the onset of discontinuous grain growth. In the latter case, discrete grains in the structure, termed secondaries, consumed the primary grain matrix resulting in the formation of a duplex structure. The incubation period for the onset of discontinuous grain growth increased with increasing boron content.

Discontinuous grain growth was postulated to be due to a combination of the dissolution of the tungsten boride phase that freed the pinned grain boundaries and the coalescence of two adjacent primary grains to form a large secondary grain.

Grain-boundary migration rates were calculated for the primary and secondary grains in all the alloys. Small amounts of boron, of the order of 0.01 atomic percent were observed to decrease the grain-boundary migration rate of tungsten by three orders of magnitude. This decrease was attributed to the segregation of boron to the grain boundaries. Larger additions of boron (greater than 0.25 atomic percent) promoted the formation of tungsten boride, which pinned the boundaries at 3600° and 3800° F. At 4000° and 4200° F, the boride partially dissolved resulting in the release of the boundaries and a subsequent increase in the grain-boundary migration rate.

### INTRODUCTION

On exposure to high temperatures, polycrystalline metals normally undergo the process of grain growth, resulting in a decrease in the grain-boundary surface area  $\beta$  and consequently the grain-boundary surface energy. (All symbols

are defined in appendix A.) [Although the kinetics of grain growth have been studied for many materials, investigations of tungsten have been limited generally to the process in powder-metallurgical lamp wires (refs. 1 to 4). [The principal results of these studies are that the grain-growth characteristics of tungsten are substantially influenced by the addition of certain alkali salts to the powder during processing. After fabrication, these are partially retained in the tungsten as trace impurities that affect both the rate of grain growth and the final grain morphology after a high-temperature anneal.]

Limited studies have been made on the annealing behavior of tungsten produced by melting processes. Klopp and Raffo (ref. 5) studied the recrystallization and grain-growth behavior of five lots of arc-melted tungsten and concluded that the wide variations observed were due to small differences in purity among the five lots. Electron-beam-melted tungsten recrystallized and exhibited rapid grain growth at temperatures well below those for arc-melted and powder-metallurgy tungsten (unpublished data obtained by W. R. Witzke of Lewis).

[The purpose of the present investigation was to study the influence of boron on the grain-growth kinetics of high-purity arc-melted tungsten. The practical justification for studying grain growth in tungsten is the effect of grain size on the high-temperature tensile and creep properties (ref. 5). Boron was considered initially as an addition that would stabilize the grain structure and thus lead to improved high-temperature strength. Clark (ref. 6) and the present authors have previously observed significant decreases in the rate of grain growth by small (less than 0.1 atomic percent) amounts of boron. The present study was aimed at examining this process over a larger range of boron contents in an attempt to characterize the mechanisms by which boron additions influence the grain-growth rate. To achieve this end, the grain-growth behavior of arc-melted tungsten and several binary tungsten-boron alloys (0.005 to 0.67 atomic percent B) was studied in the temperature range 3600° to 4200° F, corresponding to the range of interest for these materials.]

#### EXPERIMENTAL PROCEDURES

[The alloys were prepared by blending elemental tungsten and boron powders from the same batch and hydrostatically pressing them at 60 000 pounds per square inch to a  $1\frac{5}{16}$ -inch-diameter electrode. Each electrode was sintered at a pressure of less than  $5 \times 10^{-5}$  millimeter of mercury for 1 hour at 4200° F, to give a density of approximately 80 to 85 percent of theoretical, and then consumably arc-melted into a 2- or 2.68-inch-diameter water-cooled copper crucible to yield a 10- to 17-pound ingot.] The arc melting facility has been described previously (ref. 7). The ingot compositions and grain sizes are given in table I.

[Extrusion billets were machined from the ingots and extruded under the conditions given in table I.] Alloys B-1, B-2, B-3, B-4, and B-5 were impact-extruded at an 8-to-1 reduction ratio in a Dynapak extrusion press, while alloy B-6 was extruded in a conventional hydropress. Alloys B-5 and B-6 were clad with 0.100-inch molybdenum sheet prior to extruding.

TABLE I. - FABRICATION PROCEDURES FOR ALLOYS

Alloy	Boron content, atomic percent	Extrusion temperature, °F	Reduction ratio	Swaging temperature, °F	Swaging reduction, percent
B-1	0	3500	6	2650	66.8
B-2	.012	3500	8	2500	77.6
B-3	.005	3500	8	2500	77.6
B-4	.25	3500	8	2500	77.6
B-5	.59	3800	8	2700	77.6
B-6	.67	4000	6	2650	80.0

The alloys were swaged at the temperatures indicated in table I on a conventional rotary swaging machine. The molybdenum was removed from the extruded rod in alloys B-5 and B-6 prior to swaging. Heating was accomplished by induction in hydrogen by using a tungsten susceptor. The temperature was decreased with increasing reduction to maximize the amount of cold work introduced into the material. The swaging conditions are given in table I.

Specimens cut from the swaged rods were recrystallized for 1 hour at 3200° F in vacuum in a tungsten-sheet-element resistance furnace. This was done in order to insure that only grain growth took place during the subsequent anneals. The grain-growth annealing treatments were performed in a water-cooled stainless-steel shell at a pressure of less than  $10^{-5}$  millimeter of mercury. A tantalum heater was used at 3600° to 3800° F, while a heater made from meshed-tungsten wire was used at 4000° to 4200° F. Temperature was measured with an optical pyrometer sighted on a blackbody cavity near the specimens, as shown in figure 1. Temperatures were constant within 5° and are believed to be accurate to  $\pm 25^{\circ}$  F.

The specimens were suspended on a tungsten wire and quenched after each anneal by dropping them into a copper pot, as shown in figure 1. The specimen was quenched with cold helium that flowed from a perforated coil in the pot. After annealing, the specimens were sectioned longitudinally and electropolished in a 2-percent sodium hydroxide solution. Quantitative metallographic procedures, outlined in appendix B, were employed to characterize the grain sizes of the various materials.

Boron analyses were performed at a commercial laboratory by a colorimetric method involving the distillation of methyl borate. The values were stated by the laboratory as being accurate to  $\pm 10$  percent at the 5- to 400-ppm level.

## RESULTS

In order to study the grain-growth kinetics in dilute tungsten-boron alloys, fully recrystallized specimens of alloys B-1, B-2, B-3, B-4, B-5, and B-6 were annealed at 3600° to 4200° F for times of 10 minutes to 30 hours. The compositions of the alloys are given in table I. It is normal practice to employ the average grain diameter as the parameter to describe grain-growth behavior; however, discontinuous grain growth was observed in all the tungsten-boron alloys at 3600° to 4200° F resulting in the formation of a duplex grain structure. Here the concept of an average grain diameter loses its significance because of the nonuniformity of the structure, and another parameter had to be selected. The parameter selected was  $\beta$ , the grain-boundary surface area

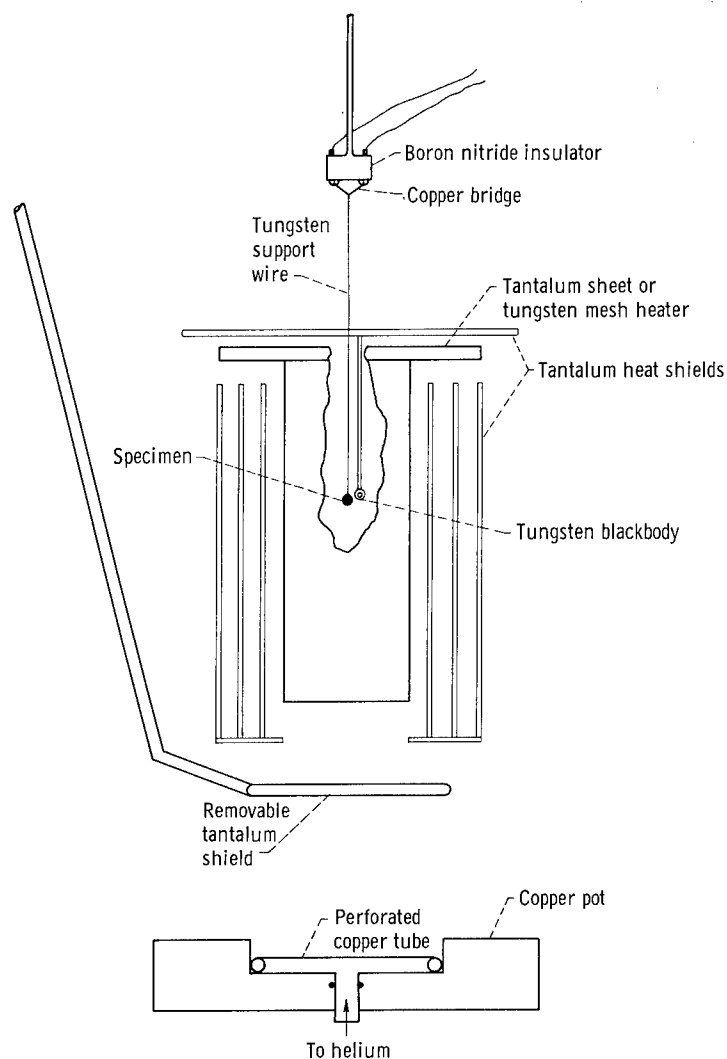


Figure 1. - Heat-treating apparatus.

per unit volume of the specimen. Details of the metallographic determination of  $\beta$  and its relation to the average grain diameter are given in appendix B.

The time dependence of  $\beta$  at 3600° to 4200° F for the materials studied is illustrated in figure 2. The error bars shown represent the standard deviation (one sigma limit) obtained from the 20 readings taken on each specimen. The percentage error is higher for the small values of  $\beta$  because of the limited number of grain boundaries available compared with the finer grained specimens.

Limited data were obtained for the unalloyed tungsten standard B-1, and the results are illustrated in figure 2(a). For the materials containing boron, certain characteristics were found for all the curves except for alloy B-2, tungsten - 0.012 atomic percent boron. At 3600° to 3800° F, the data for alloy B-2 fit an equation of the form

$$\beta = kt^{-n}$$

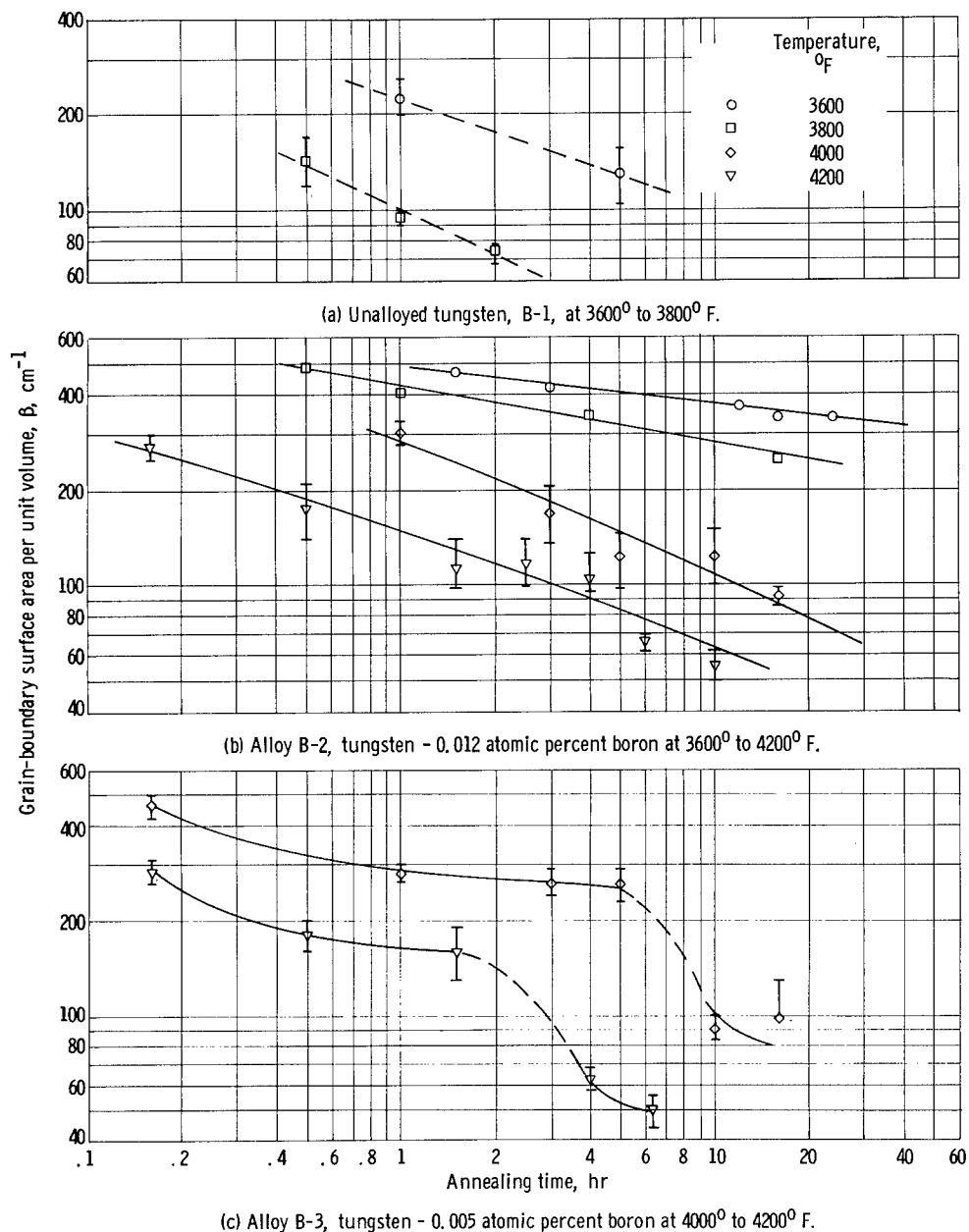
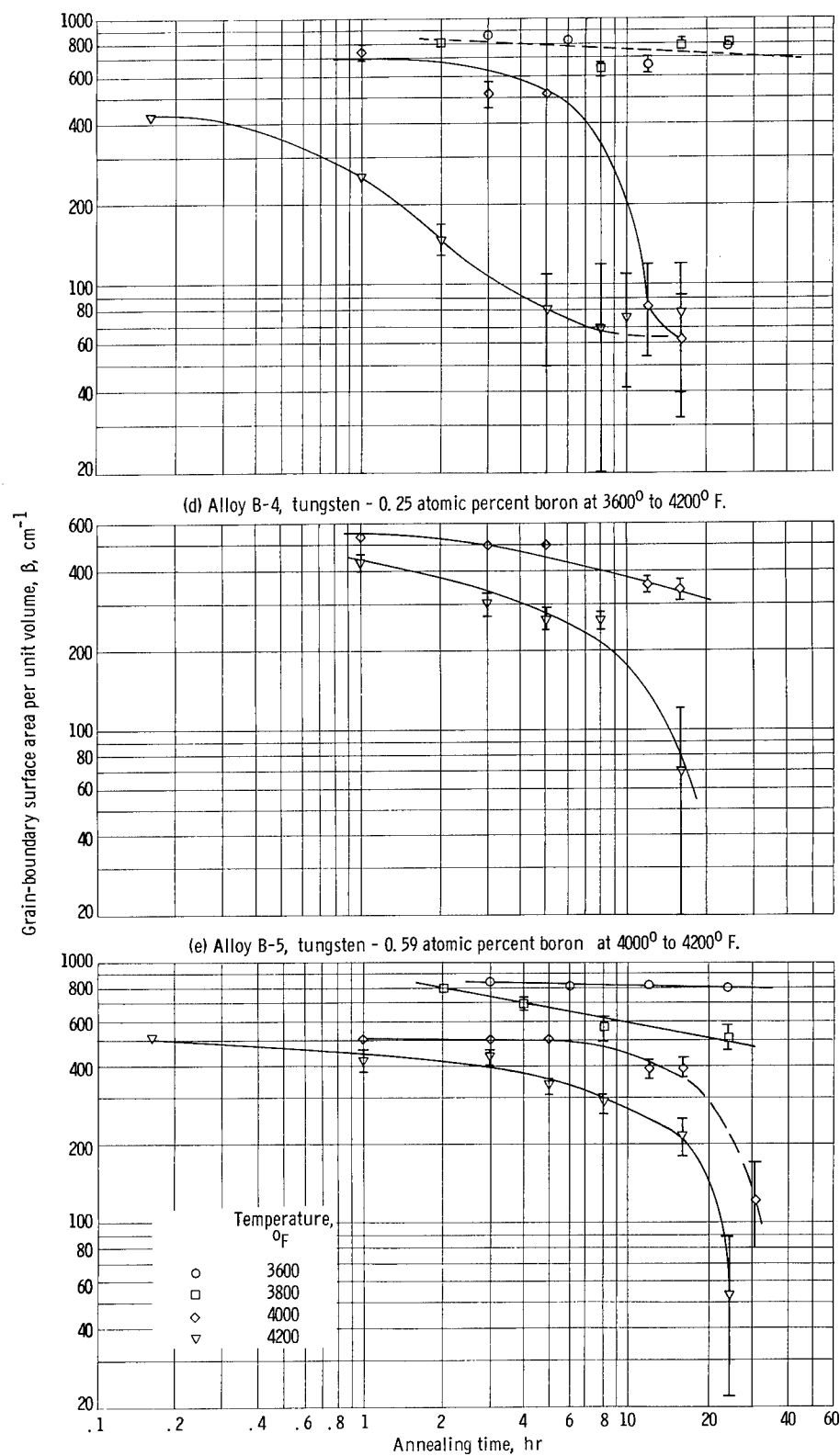


Figure 2. - Grain-growth behavior.

where  $k$  and  $n$  are constants. The values of  $n$  ranged from 0.121 at 3600° F to 0.183 at 3800° F. This is considerably less than the theoretical value of 0.5 for ideal grain growth as determined by Feltham (ref. 8). At 4000° and 4200° F, the relation was no longer obeyed due to the initiation of discontinuous grain growth. In this case, discrete grains in the structure (secondaries) grew from the primary grain structure resulting in the formation of a duplex structure; an example is shown in figure 3. The result was to produce a more rapid decrease in  $\beta$  due to the formation and rapid growth of these secondaries. The rate of decrease of  $\beta$  at 4000° and 4200° F approached a  $t^{1/2}$  law if a straight line were to be drawn through the points; however, such a re-





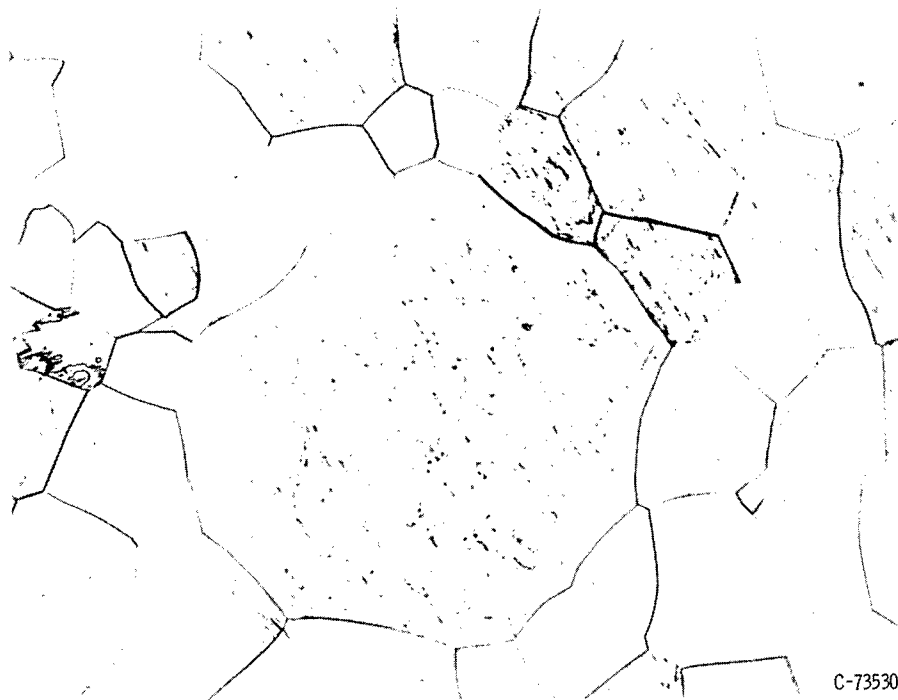


Figure 3. - Alloy B-3 showing example of discontinuous grain growth. Annealed at 4200° F for 1/2 hour; etchant, boiling 3-percent hydrogen peroxide. X150.

lation should only be expected when uniform grain growth takes place, and this was not observed in the present case. Similar behavior was noted for alloy B-3 at these temperatures (fig. 2(c)), but a much more distinct transition to discontinuous grain growth was observed.

Figures 2(d) to (f) illustrate the isothermal behavior of the high-boron alloys B-4, 0.25 atomic percent boron; B-5, 0.59 atomic percent boron; and B-6, 0.67 atomic percent boron. At 4000° to 4200° F, the shape of the curves for logarithm of  $\beta$  against logarithm of  $t$  was similar to that observed for alloy B-3, except that the time for the onset of discontinuous grain growth increased with increasing boron content. It was also observed that the error in small values of  $\beta$  for the high-boron alloys was greater due to the greater nonuniformity of the structure.

Comparison of the data for the dilute boron alloys with that of the unalloyed tungsten standard B-1 revealed that the alloys exhibited considerably slower growth rates at 3600° and 3800° F. Metallographic examination of the materials indicated that a second phase, presumably tungsten boride ( $W_2B$ ), was present in alloys B-4, B-5, and B-6, while none was observed in the other alloys.

#### DISCUSSION

The two important aspects of the current results are (1) the observation of discontinuous grain growth and its dependence on boron content and (2) the

differences in growth rates among the alloys. The first section of the discussion describes the nucleation of the secondary grains in the tungsten-boron alloys and relates it to the existing theories of discontinuous grain growth. Secondly, the grain-boundary migration rates of the primary and secondary grains are calculated in order to make comparisons with respect to the boron content.

### Discontinuous Grain Growth

An important result of this study was the observation that an increase in the boron content caused an increase in the time for the initiation of discontinuous grain growth. Beck, et al. (ref. 9) and May and Turnbull (ref. 10) here attributed the start of discontinuous grain growth to the dissolution or coalescence of impurity phases that inhibit grain growth at the lower temperatures. May and Turnbull stated this formally by representing the net driving force for grain growth  $\Delta F_G$  as

$$\Delta F_G = P - I \quad (1)$$

where  $P$  is the driving force tending to increase the grain size and  $I$  is a restraining factor dependent upon the size and volume fraction of the impurity phase particles (ref. 9). When  $I$  decreases or becomes zero, the net driving force increases and the grains grow more rapidly. In the present investigation, visible second-phase particles were observed in the higher boron alloys, and the incubation period for initiation of discontinuous grain growth increased with an increase in the volume fraction of the boride. This is in agreement with equation (1), since the larger volume fraction would increase the inclusion factor  $I$  and hence lengthen the time for the driving-force term to overcome it.

Although the importance of having a restraining factor as a prerequisite for discontinuous grain growth is well established (refs. 9 and 10), the conditions for the formation of a large secondary grain capable of rapid growth are not. Intuitively, one might expect the entire structure to coarsen uniformly as the impurity phases dissolved or coalesced. Instead, discrete grains nucleate and consume the primary grain structure suggesting that, if dissolution takes place, it is highly localized. Nielsen (ref. 11) in 1954 advanced an alternative explanation of the origin of secondary grains in which the concept of "geometrical" coalescence was introduced. Essentially, this theory states that pairs of nearby grains of approximately the same orientation may meet along a grain edge and coalesce as a result of some local instability of the grain structure. The local instability is that the grain boundaries that intersect along the edge are of high surface energy, but the resultant surface tension at the intersection is nearly zero. Thus, these boundaries may move apart resulting in the coalescence of the two grains of similar orientation. The resulting coalesced grain now has a larger number of sides in addition to its larger volume. The larger number of sides have been shown by Neumann (ref. 11) to be sufficient for rapid growth of the secondary grains. Geometric coalescences have been observed in the present study in the early annealing stages of alloys B-2 and B-3 at 4000° F. Examples for B-3 are shown in figure 4.



Figure 4. - Examples of geometric coalescence found in alloy B-3. Grains A and B coalesced because of outward movement of grain boundaries LMN and RST. Annealed at 4200° F for 30 minutes; etchant, boiling hydrogen peroxide solution. X150.

The results of the present investigation appear to be in qualitative agreement with both theories of discontinuous grain growth. The data suggest that, although particle dissolution is an important factor in determining the nucleation of secondary grains, some other process such as geometric coalescence might be a necessary intermediate step in the formation of a secondary. Additional data should be obtained to substantiate this point.

#### Grain-Boundary Migration Rates

In the preceding paragraphs, the possible mechanism for nucleation of secondary grains was discussed. An attempt was also made to study the boundary migration rates of the primaries and secondaries in an effort to determine their dependence on driving force, temperature, and boron content.

The boundary migration rates  $G_i$  were calculated from the data by the equation

$$G_i = \frac{dD_i}{dt} \quad (2)$$

where  $D_i$  is the average primary or secondary grain diameter. The primary grain diameter and the secondary grain diameter were calculated as shown in appendix B. Figure 5 shows representative plots of primary grain diameter  $D_p$  and secondary grain diameter  $D_s$  against time for selected alloys at 4000°

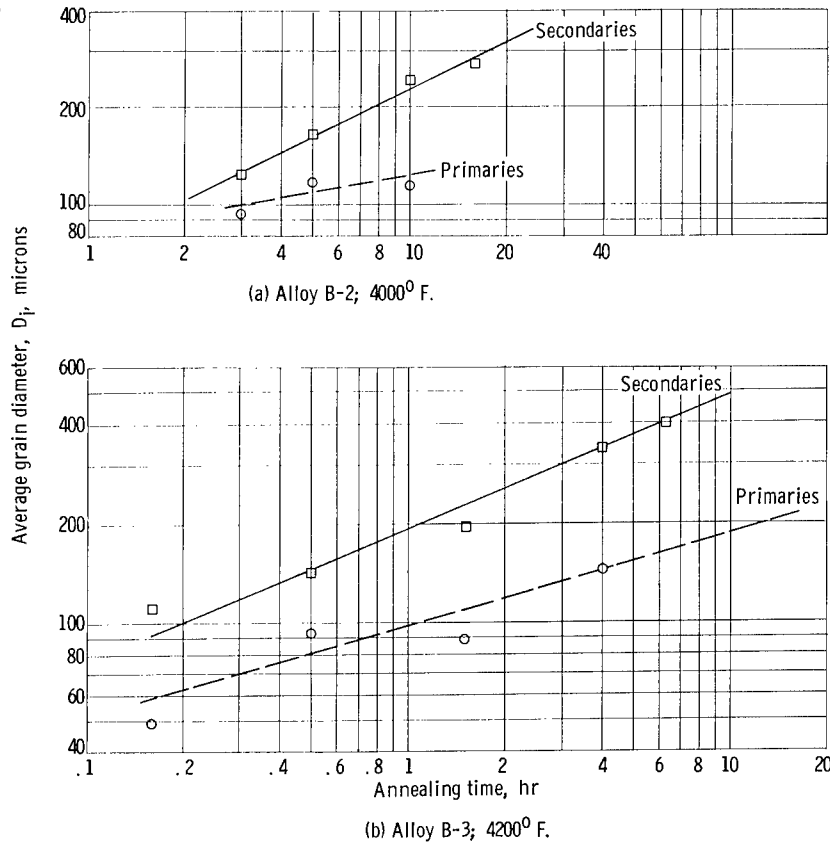


Figure 5. - Growth of primary and secondary grains.

and 4200° F. Although the scatter in the data varied among the materials, it was felt that the time dependence of the average grain diameters could be reasonably well represented by the power law

$$D_i = k_i t^n$$

Differentiating gives

$$G_i = \frac{dD_i}{dt} = nk_i t^{n-1}$$

Employing the constants  $n$  and  $k_i$  determined by the least-squares method gives a value of  $G_i$  for both the primary and secondary grains as a function of time. The data for alloys B-4 and B-6 were limited because of the rapid growth of the secondaries in a short time span that allowed only a few values of  $D_s$  to be calculated.

Examination of figure 5 revealed the important observation that, during the discontinuous grain growth of these alloys, both the primary and secondary grains grow, but at different rates. This should result in  $G_s$  decreasing with time, since the driving force  $\beta_p$  also decreases with time. This observation was borne out by actual calculation of  $G_s$ .

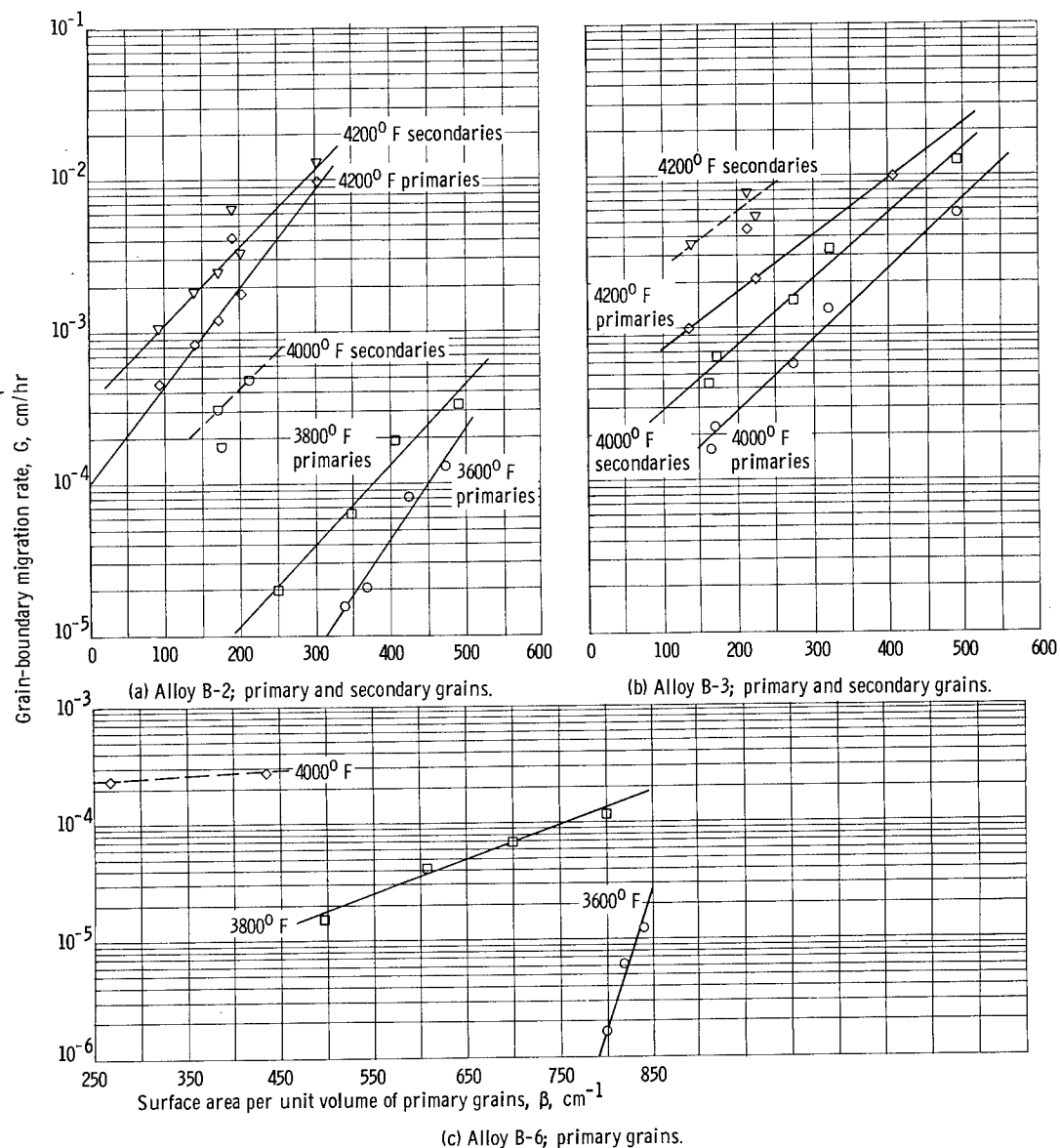


Figure 6. - Driving-force dependency of grain-boundary migration rate.

### [Impurity Effects on Grain-Boundary Migration]

The grain-boundary migration rates calculated in the previous section should depend upon the temperature  $T$ , the driving force  $P$ , and the solute content  $C$  (ref. 12). One can mathematically illustrate these effects by the equation

$$dG = \frac{\partial G}{\partial P} dP + \frac{\partial G}{\partial T} dT + \frac{\partial G}{\partial C} dC \quad (3)$$

where the total differential of  $G$  is written as a function of driving force, temperature, and composition dependencies. If the migration rate  $G$  can be

evaluated at a constant driving force and temperature ( $dP = dT = 0$ ) the composition effect can be determined. The purpose of this discussion is to determine the influence of these variables on grain growth in the present alloys.

In the present work,  $G$  was calculated from equation (2) for alloys B-1, B-2, B-3, B-4, and B-6 and then plotted against the proper value of  $\beta_p$ , the grain-boundary surface area per unit volume of the primaries. A linear relation, as suggested previously (ref. 8) for ideal grain growth, was initially attempted, but a poor fit resulted. Semilogarithmic plots of  $G$  against  $\beta_p$  were then made and are illustrated in figure 6. The data fit an equation of the form

$$G = A \exp(-\alpha\beta_p) \quad (4)$$

and where sufficient data were available, a least-squares analysis of the data gave a good fit with determination coefficients of 97 to 99.5 percent.

The temperature dependence of the grain-boundary migration rate was found by plotting  $G$  on an Arrhenius plot at a constant driving force ( $\beta_p = 300 \text{ cm}^{-1}$ ) as shown in figure 7. The boundary migration rates for the primary grains in alloys B-2 and B-3 fell on the same curve within the accuracy of the calculations of  $G$ . On the other hand, the values of  $G$  for the unalloyed standard B-1, at a given temperature, were three orders of magnitude higher, while those for the high-boron alloy B-6 were lower. Since these comparisons are made at a constant temperature and driving force, the differences must be related to composition according to equation (3).

The temperature dependence of the grain-boundary migration rate at a constant driving force has been written as (ref. 8)

$$G = G_0 \exp(-H/RT)$$

where  $H$  is the activation energy and  $G_0$  is a constant. The activation energy  $H$  was evaluated from figure 7 for alloys B-2 and B-3 and found to be 244 kilocalories per mole. It has been suggested previously that  $H$  is equal to the activation energy for grain-boundary self-diffusion (ref. 8), but the present value is even considerably larger than that for volume self-diffusion in tungsten of 153 kilocalories per mole (ref. 13). Impurities have been shown previously to increase the activation energy (ref. 14); however, the present value still appears to be too large. The discrepancy here might be due to one of two reasons: either the migration rates calculated herein do not represent the single process of grain-boundary migration or an undefined competing process is taking place that would limit the use of an Arrhenius representation.

It appears then, that the large differences in the grain-boundary migration rates among the alloys are related to composition. Of importance, is the mechanism by which the impurities, in particular boron, restrain grain growth. The solubility of boron in tungsten is small and of the order of 0.2 atomic percent at  $4532^\circ \text{ F}$  and 0.1 atomic percent at  $1832^\circ \text{ F}$  (ref. 15). Therefore, one would expect boron to be in solution in alloys B-1, B-2, and B-3 at all tem-

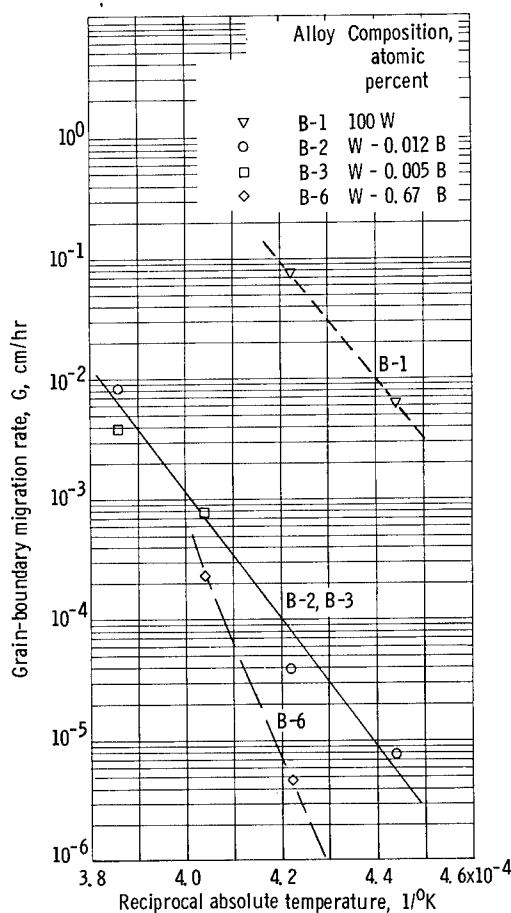


Figure 7. - Temperature dependence of grain-boundary migration rate evaluated at grain-boundary surface area per unit volume of primaries of 300 per centimeter.

peratures and to be partially dissolved in the higher boron alloys. Thus, the curve in figure 7 for the tungsten - 0.67-atomic-percent-boron alloy presumably represents two competing processes, that for movement of the grain boundary and that for dissolution of the boride phase. The fine particles that prohibit grain-boundary migration at the low temperatures dissolve at the higher temperatures, thus increasing the boundary migration rate.

It is not clear, however, as to the manner in which the small additions of boron in alloys B-2 and B-3 can lower the value of  $G$  by three orders of magnitude with respect to the unalloyed tungsten standard B-1. A considerable amount of experimental and theoretical work (refs. 12, 14, 16, 17, and 18) has revealed that solute additions of this magnitude strongly decrease the grain-boundary migration rate. This effect arises from the equilibrium segregation of the solute atoms to the grain boundaries. When the boundary moves away from the solute atoms, the local equilibrium is destroyed and the solute atoms diffuse back to the boundary to restore it. This diffusion behind the boundary constitutes a drag on its further motion. The drag increases as the velocity increases (ref. 12) and passes through a maximum at high velocities. Lücke and Stüwe (ref. 12) have demonstrated that

the drag force is proportional to the driving-force dependency such that the latter term might be expected to increase with velocity also. This was observed in the present work, since differentiation of equation (4) to find  $\partial G / \partial P$  leads to a linear relation with  $G$  in qualitative agreement with the expectations of Lücke and Stüwe.

Segregation of solutes to grain boundaries has been observed in other metals. Aust and Rutter observed that local segregation of tin (ref. 14), silver, and gold (ref. 16) produced pronounced lowering of the grain-boundary migration rate in zone-refined lead bicrystals. Westbrook and Aust (ref. 19) in a later paper verified the result by illustrating pronounced grain-boundary hardening due to the segregated solutes in the same bicrystals. Boron would be expected to segregate strongly to the grain boundaries in tungsten because of the large atomic size difference (ref. 18), but an accurate indication of the segregation tendency is not known. The calculations in appendix C show that the boron in solution in alloys B-2 and B-3 is sufficient to saturate the grain boundaries at these temperatures. Thus, boron in this composition range would be expected to give the pronounced effect noted on the grain-boundary migration rate.

TABLE II. - REPRESENTATIVE CHEMICAL  
ANALYSES OF SWAGED MATERIALS

Element	Impurities, ppm					
	Alloy					
	B-1	B-2	B-3	B-4	B-5	B-6
Carbon	14	4	3	5	5	9
Nitrogen	13	6	11	5	8	10
Oxygen	3	6	11	5	8	4
Aluminum	10	13	15	3	3	10
Calcium	10	10	20	<sup>a</sup> <10	10	10
Copper	7	<1	10	<1	5	3
Iron	10	10	28	10	20	20
Molybdenum	10	10	30	10	20	20
Silicon	<20	<20	<20	7	10	10

<sup>a</sup>Not detected, i.e., less than value indicated.

The influence of other trace impurities should not be ignored, however. Other investigators have shown the strong influence of elements such as iron, silicon, and aluminum in decreasing grain-boundary migration in tungsten (ref. 5). Spectrographic analyses of the alloys shown in table II did not reveal any large differences in the amounts of these impurities. These arguments can be used to draw the tentative conclusion that the boron additions caused the differences in the grain-boundary migration rates and that the boron in solution is the predominant influence.

#### SUMMARY OF RESULTS

This study of the kinetics of grain growth in dilute tungsten-boron alloys produced the following results:

1. The decrease in the grain-boundary surface area per unit volume of dilute tungsten-boron alloys at 3600° and 3800° F followed a relation in the form

$$\beta = kt^{-n}$$

while at 4000° and 4200° F, discontinuous grain growth occurred and caused a much larger decrease with time.

2. The incubation time for discontinuous grain growth increased with increasing boron content. The cause of the discontinuous grain growth was related to geometric coalescence of adjacent grains and particle dissolution at the grain boundaries.

3. The grain-boundary migration rate, evaluated at a constant temperature and driving force, decreased sharply with additions of less than 0.012 percent boron. Additions of boron greater than this amount caused an additional de-



crease at 3600° to 3800° F, but their influence lessened with increasing temperature due to the dissolution of fine boride particles that restricted growth at the lower temperatures.

Lewis Research Center,  
National Aeronautics and Space Administration,  
Cleveland, Ohio, December 14, 1964.

## APPENDIX A

### SYMBOLS

A	total atoms per unit volume
$a_f$	atomic fraction of solute in material
$b^3$	atomic volume, cu cm
C	total solute concentration
$C_g$	grain-boundary concentration
$C_o$	lattice concentration
$D_i$	average grain diameter, $\mu$
$\Delta F_G$	net driving force for grain growth
$f_i$	volume fraction of primary or secondary grains
$G_i$	grain-boundary migration rate, cm/hr
H	activation energy for grain growth
I	restraining factor dependent on size and volume fraction of impurities
L	length of line
M	molecular weight of tungsten, 183.86 g/mole
N	number of intercepts
$N'$	number of solute atoms in lattice per unit volume
$\bar{N}$	Avogadro's number, $6.023 \times 10^{23}$ atoms/mole
n	number of solute atoms in grain boundary per unit volume
P	driving force for grain growth
p	number of lattice sites in grain boundary per unit volume
$p'$	number of sites in grain boundary per unit volume
R	gas constant, 1.98 cal/mole/ $^{\circ}$ K
r	atomic radius of solvent atom
$r'$	radius of solute atom

$S$  total grain-boundary surface area  
 $T$  temperature  
 $t$  time  
 $U$  interaction energy of solute with grain boundary  
 $V$  volume of sample  
 $x$  boundary thickness  
 $y$  temperature dependent segregation factor  
 $\alpha$  proportionality factor  
 $\beta$  grain-boundary surface area per unit volume,  $\text{cm}^{-1}$   
 $\mu$  shear modulus  
 $\rho$  density of tungsten,  $19.3 \text{ g/cu cm}$   
 $\Sigma$  misfit factor,  $(r' - r)/r$   
 $\sigma$  Poisson's ratio

Subscripts:

$i$  primary or secondary  
 $p$  primary  
 $s$  secondary

## APPENDIX B

### QUANTITATIVE METALLOGRAPHIC PROCEDURES

#### TO CHARACTERIZE GRAIN SIZES

The microstructure of a polycrystalline metal is quantitatively specified if the size and amount of the various constituents are known. The methods of quantitative metallography involve the determination of these quantities by measurements on a random plane section through a metal or an alloy (ref. 20). Expressions employing quantitative metallography are needed to calculate the average dimensions of the individual grains in the material. An expression is also needed to differentiate between the sizes of the secondary and primary grains in a duplex structure undergoing discontinuous grain growth.

Consider the superposition of a line of any shape on the plane section of the etched specimen. The total grain-boundary surface area  $S$  per unit volume of the sample  $V$ , is equal to (ref. 20)

$$\beta = \frac{S}{V} = \frac{2N}{L} \quad (B1)$$

where  $N$  is the number of intercepts that the boundaries make with a line of length  $L$ . Similarly in a duplex structure, the grain-boundary surface area surrounding the secondary grains  $S_s$  per unit volume of the secondaries  $V_s$  can be expressed as (ref. 20)

$$\beta_s = \frac{S_s}{V_s} = \frac{2N_s}{L_s} \quad (B2)$$

where  $N_s$  is the number of intercepts that the secondary grain boundaries make with the total length of line  $L$ , and  $L_s$  is the fraction of the length  $L$  that lies in the secondaries. The volume fraction of the secondaries  $f_s$  is also given by

$$f_s = \frac{L_s}{L} = \frac{V_s}{V} \quad (B3)$$

For the primary grains, similar quantities exist:

$$\beta_p = \frac{S_p}{V_p} \quad (B4)$$

The average size of the individual grains may now be calculated. The secondary grain diameter  $D_s$  is (ref. 21)

$$D_s = \frac{2}{\beta_s} \quad (B5)$$

and the primary grain diameter  $D_p$  is

$$D_p = \frac{2}{\beta_p}$$

In order to minimize the number of measurements needed to calculate  $D_s$  and  $D_p$ , a relation was found between  $\beta_p$  and  $\beta$  as shown subsequently.

In the early stages of discontinuous grain growth

$$S_p = S \quad (B6)$$

providing that each secondary is completely surrounded by primaries. Then combining (B4) and (B6) and multiplying by  $V/V_p$  yield

$$\beta_p = \frac{S_p}{V_p} = \frac{S}{V_p} = \frac{S}{V} \times \frac{V}{V_p} = \frac{\beta}{f_p} \quad (B7)$$

where  $f_p$  is the volume fraction of the primaries and is equal to  $1 - f_s$ . Thus,

$$D_p = \frac{2}{\beta_p} = \frac{2(1 - f_s)}{\beta} \quad (B8)$$

For  $f_s = 0$  (uniform grain size), equation (B8) becomes

$$D_p = \frac{2}{\beta} = \frac{L}{N} \quad (B9)$$

which is the standard ASTM relation for the determination of grain size.

## APPENDIX C

### CALCULATION OF CONDITIONS FOR BORON SATURATION OF HIGH ANGLE GRAIN BOUNDARIES IN TUNGSTEN

McLean (ref. 22) gives

$$C_g = \frac{yC_o}{1 + yC_o} \quad (C1)$$

as the grain-boundary concentration. The concentration terms  $C_g$  and  $C_o$  are given most conveniently in terms of the number of solute atoms per grain boundary or lattice site. Thus

$$A = \frac{\bar{N}_o}{M}$$

$$N' + n = a_f A$$

and

$$p = \frac{1}{b^3}$$

so that the lattice concentration becomes equal to

$$C_o = \frac{N'}{p} = (a_f A - n)b^3 \quad (C2)$$

The number of grain-boundary sites per unit volume is given as (ref. 22)

$$p' = \frac{\beta x}{b^3}$$

At saturation, some fraction  $a$  of these sites is filled; thus, the number of solute atoms in the grain boundary under these conditions is

$$n = a \frac{\beta x}{b^3} \quad (C3)$$

Thus,

$$C_g = \frac{n}{p'} = a$$

at saturation. McLean (ref. 22) assumes that approximately one-third of the sites are filled when the boundary is saturated. These assumptions can be used

to rewrite equation (C1) in the following form:

$$\frac{1}{3} = \frac{\left[ a_f A - \frac{1}{3} \left( \frac{\beta x}{b} \right) \right] b^3 y}{1 + \left[ a_f A - \frac{1}{3} \left( \frac{\beta x}{b} \right) \right] b^3 y} \quad (C4)$$

The segregation factor  $y$  is given by

$$y = \exp \frac{U}{RT}$$

where  $U$  is the interaction energy of a solute with a grain boundary. Lücke and Stuwe (ref. 12) suggest a number of ways of calculating  $U$ . In this study, the Cottrell formula was used

$$U = \frac{4}{3} \frac{(1 + \sigma)}{(1 - \sigma)} r^3 \mu \Sigma$$

The values for the tungsten-boron system were used to calculate  $U$ , which was 37.56 kilocalories per mole for boron in tungsten. The segregation factor  $y$  was then calculated in the temperature range 3600° to 4200° F, and the atomic fraction  $a_f$  necessary to saturate the grain boundaries was evaluated from equation (C4) for  $\beta = 100$  to 400. The values of  $a_f$  varied from  $9.8 \times 10^{-5}$  to  $2.34 \times 10^{-4}$  (0.0098 to 0.0234 atomic percent), which is within the range of boron contents existing in the low-boron alloys B-2 and B-3.

## REFERENCES

1. Swalin, R. A., and Geisler, A. H.: The Recrystallization Process in Tungsten as Influenced by Impurities. *Inst. Metals Jour.*, vol. 86, Nov. 1957, pp. 129-134.
2. Rosi, Fred D.: Orientation Studies of Exaggerated Grain Growth in Tungsten. *Sylvania Technologist*, vol. 5, Oct. 1952, pp. 82-86.
3. Meijering, J. L., and Rieck, G. D.: The Function of Additives in Tungsten for Filaments. *Phillips Tech. Rev.*, vol. 19, no. 4, 1957-58, pp. 109-117.
4. Mannerkoski, M.: The Effect of Temperature and Heating Rate on the Secondary Recrystallization of Doped Tungsten Wires. *Inst. Metals. Jour.*, vol. 92, Jan. 1964, pp. 149-150.
5. Klopp, W. D., and Raffo, P. L.: Effects of Purity and Structure on Recrystallization, Grain Growth, Tensile and Creep Properties of Arc-Melted Tungsten. NASA TN D-2503, 1964.
6. Clark, J. W.: Flow and Fracture of Tungsten and Its Alloys: Wrought, Recrystallized, and Welded Conditions. ASD-TDR-63-420, General Electric Co., Apr. 1963.
7. Foyle, F. A.: Arc Melted Tungsten and Tungsten Alloys. *High Temperature Materials*, Pt. II, Vol. 18, Intersci. Pub., 1963, pp. 109-124.
8. Feltham, P.: Grain Growth in Metals. *Acta Metallurgica*, vol. 5, Feb. 1957, pp. 97-105.
9. Beck, Paul A., Holzworth, M. L., and Sperry, Philip R.: Effect of a Dispersed Phase on Grain Growth in Al-Mn Alloys. *Trans. AIME*, vol. 180, 1949, pp. 163-192.
10. May, John E., and Turnbull, David: Secondary Recrystallization in Silicon Iron. *Trans. AIME*, vol. 212, Dec. 1958, pp. 769-782.
11. Nielsen, John P.: Mechanism for the Origin of Recrystallization Nuclei. *Trans. AIME*, vol. 200, Sept. 1954, pp. 1084-1088.
12. Lücke, Kurt, and Stüwe, Hein-Peter: On the Theory of Grain Boundary Motion. Recovery and Recrystallization of Metals, Intersci. Pub., 1963.
13. Andelin, Robert L.: Self-Diffusion in Single-Crystal Tungsten and Diffusion of Rhenium Tracer in Single-Crystal Tungsten. LA-2880, Los Alamos Sci. Lab., Mar. 1963.
14. Aust, K. L., and Rutter, J. W.: Temperature Dependence of Grain Migration in High-Purity Lead Containing Small Additions of Tin. *Trans. AIME*, vol. 215, Oct. 1959, pp. 820-831.



15. Goldschmidt, H. J.: Investigation into the Tungsten-Rich Regions of the Binary Systems Tungsten-Carbon, Tungsten-Boron and Tungsten-Beryllium. ASD-TDR-62-25, Pt. II, B.S.A. Res. Centre, Kitts Green, Birmingham (Gt. Britain), July 1963.
16. Rutter, J. W., and Aust, K. T.: Kinetics of Grain Boundary Migration in High-Purity Lead Containing Very Small Additions of Silver and Gold. Trans. AIME, vol. 218, Aug. 1960, pp. 682-688.
17. Bolling, G. F., and Winegard, W. C.: Some Effects of Impurities on Grain Growth in Zone-Refined Lead. Acta Metallurgica, vol. 6, no. 4, Apr. 1958, pp. 283-287.
18. Lucke, K., and Detert, K.: A Quantitative Theory of Grain-Boundary Motion and Recrystallization in Metals in the Presence of Impurities. Acta Metallurgica, vol. 5, Nov. 1957, pp. 628-637.
19. Westbrook, J. H., and Aust, K. T.: Solute Hardening at Interfaces in High-Purity Lead. I - Grain and Twin Boundaries. Acta Metallurgica, vol. 11, Oct. 1963, pp. 1151-1163.
20. Smith, Cyril Stanley, and Guttman, Lester: Measurement of Internal Boundaries in Three-Dimensional Structures by Random Sectioning. Jour. Metals, vol. 5, no. 1, Jan. 1953, pp. 81-87.
21. Cremens, W. S.: Use of Sub-Micron Metal and Non-Metal Powders for Dispersion-Strengthened Alloys. Ultrafine Particles, W. E. Kuhn, ed., John Wiley & Sons, Inc., 1963, pp. 457-478.
22. McLean, D.: Grain Boundaries in Metals. Clarendon Press (Oxford), 1957.